FREQUENCY DOMAIN STUDIES OF IMPEDANCE CHARACTERISTICS OF BIOLOGICAL CELLS USING MICROPIPET TECHNIQUE

I. Erythrocyte

S. TAKASHIMA, K. ASAMI, AND Y. TAKAHASHI
Department of Bioengineering, University of Pennsylvania, Philadelphia, Pennsylvania 19104-6392

ABSTRACT This study aims at precise measurement of the membrane capacity and its frequency dependence of small biological cells using the micropipet technique. The use of AC fields as an input signal enables the magnitude and phase angle of membrane impedance to be measured at various frequencies. The micropipet technique was applied to human erythrocyte, and passive membrane capacity and conductivity were determined between 4 Hz and 10 KHz. Membrane capacity thus determined changed from 1.05 to 0.73 $\mu F/cm^2$ between 4 Hz and 10 KHz. In addition to the micropipet technique, we used suspension method between 50 KHz and 10 MHz for the purpose of supplementing the new method with the one which has been in use for many years. We obtained a membrane capacity of 0.65–0.8 $\mu F/cm^2$ using this technique. These values agree with the capacitance obtained with the micropipet method. Although this paper discusses only human erythrocytes, the study has been performed with lymphocytes and various forms of cancer cells. This paper is the first of the series of reports on frequency domain studies of the impedance characteristics of various biological cells.

INTRODUCTION

There are a variety of techniques for studying the impedance characteristics of small biological cells such as nerve and muscle fibers. The internal electrode and vaseline or sucrose gap techniques are the most direct and most frequently used methods for these preparations (see Tasaki, 1982; Hille and Campbell, 1976; Julian et al., 1962). For small nearly spherical cells, however, these techniques cannot be used because of their small sizes and "awkward" geometry. Traditionally, what is commonly known as the suspension technique has been used to investigate the membrane electrical properties of these cells (Schwan, 1957, 1963; Hanai et al., 1979; Asami et al., 1976). In this technique, the dielectric constant and conductivity of cell suspensions are measured. Based on these data, membrane properties are extracted using appropriate mixture equations. This method has been very effective for the investigation of electrical properties of a variety of biological cells.

Using this technique, membrane capacitances of various biological cells have been found to be ~0.8–1.0 $\mu F/cm^2$. Despite the success of this technique for the determination of membrane capacity, the suspension method has been unable to provide information on the conductance of biological membranes. Passive membrane conductances of biological cells are in general very small. For example, the anion conductance of erythrocyte membranes is known to be between 10^{-5} and 3×10^{-7} S/cm^2 for human and amphiuma red cells (Lassen et al., 1978; Hunter, 1977; Tosteson et al., 1973). This unusually small conductance cannot be detected, even with improved measuring techniques, by the suspension method. With the advent of patch clamp techniques (Sakmann and Neher, 1983), we are now able to investigate the transport properties of small biological cells in great detail. Not only the bulk membrane conductances but also single channel conductances can be studied using this technique. Membrane capacitances of various cells have also been measured using the transient current, under voltage clamp conditions, in response to step pulses. The membrane capacitance obtained by this method is, in principle, a static capacitance and does not contain much information about the dynamic properties of biological membranes. In this research, using micropipets and AC voltages as input signals, membrane capacitance and conductance of human erythrocyte and several other biological cells were investigated. The micropipet method can be used for a frequency range between 4–5 Hz and 10 KHz. The simple experimental arrangement which we will discuss later enables us to measure the impedance function between 4 and 700 Hz. In addition, a bridge technique was

Dr. Asami's permanent address is Institute for Chemical Research, Kyoto University, Uji, Kyoto, Japan.
Dr. Takahashi's permanent address is Olympus Optical Company, Hachioji Tokyo, Japan.

used for the frequency range between 300 Hz and 10 KHz.

Experimental Methods

In this research, as mentioned, two methods were used to determine the capacitance and conductance of the red cell membrane. One is the micropipet technique and the other is the suspension method.

Micropipet Technique. Micropipets were fabricated in the same way as for patch clamp measurements. The capacitance and resistance of fire polished micropipets are 2–3 pF and 40–50 MΩ, respectively. The measurements of cell impedance were performed with the "whole cell" configuration. The resistance of erythrocyte is of the order of 20–30 GΩ and the capacitance increment over that of pipet is 1.3–1.6 pF. The pipet impedance was measured twice before and after experiments in order to ensure the invariance of the pipet capacitance during measurements. Not infrequently, however, the pipet capacitance increases after cell attachment. In these cases, the second pipet readings were used as a baseline and subtracted from the total capacitance.

The measurements of capacitance and conductance were performed manually using a system illustrated schematically in Fig. 1. The feedback resistance is 214 MΩ and its parasitic capacitance was determined carefully using an impedance analyzer. The value was found to be 0.9 pF and is nearly constant over the frequency range of interest. The capacitance and conductance are given by the following equations:

$$C_p = [(V_o/V_i)C_f \cos\theta - (V_o/V_i)G_f \sin\theta/\omega] \quad (1)$$

$$G_p = [(V_o/V_i)G_f \cos\theta + (V_o/V_i)\omega C_f \sin\theta], \quad (2)$$

where V_i and V_o are input and output voltages and θ is the phase angle between them. G_f and C_f are the conductance and parasitic capacitance of feedback resistor. These measurements were carried out using an input voltage of ±30 mV. We found that the values of capacitance and conductance were independent of input voltages between ±10 mV to almost ±100 mV. Therefore, the input voltage of this magnitude has no damaging effect on erythrocyte membrane nor does it produce a nonlinear behavior.

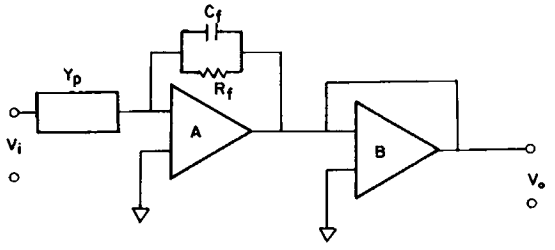

FIGURE 1 The circuit used for the measurement of membrane capacitance and conductance. (*A* and *B*) Operational amplifiers (Teledyne Philbrick 1026). R_f is a feedback resistor and C_f is parasitic capacitance.

Accurate measurements of capacitance and conductance, using the system mentioned above, become difficult above 400–500 Hz, and a conventional bridge technique had to be employed between 300 Hz and 10 KHz using a Wayne Kerr low frequency admittance bridge B221 with a model 124 PAR Lockin Amplifier. The description of this bridge is found in previous papers (Takashima and Schwan, 1974). The resolution of this bridge is sufficiently high to detect the capacitance smaller than 0.1 pF in the frequency range between 500 Hz and 10 KHz. The effect of a series resistance which is mainly due to pipet tip impedance can be easily detected around 5–10 KHz and corrected using a simple computer program. The series resistance due to cytoplasm is negligibly small compared with tip resistance and was ignored (see Fig. 2).

The major obstacle of micropipet technique is the difficulty in forming a tight seal between pipet tip and erythrocyte membrane. It is, therefore, important to investigate the effect of leakage resistance on the membrane capacitance and conductance using an equivalent circuit. A micropipet attached to a cell is depicted schematically in Fig. 2 (*inset*). Based on this arrangement, an equivalent circuit of membrane admittance including leakage and series resistances (R_L and R_s) is shown in Fig. 2. Using this circuit, the following equations for measured capacitance C_p and conductance G_p can be derived.

$$C_p = \left[\frac{C_m R}{R_s + R} - \frac{R_s R\, C_m}{(R_s + R)^2}\right] / L(\omega) \quad (3)$$

$$G_p = \left[\frac{1}{R_s + R} + \frac{\omega^2 C_m^2 R_s R^2}{(R_s + R)^2}\right] / L(\omega), \quad (4)$$

where R_s is series resistance and $L(\omega)$ is given by

$$L(\omega) = 1 + (\omega T)^2 \quad (5)$$

and

$$T = \frac{R_s R\, C_m}{R_s + R}. \quad (6)$$

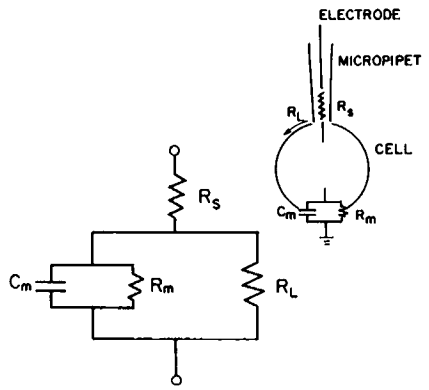

FIGURE 2 (*A*). Equivalent circuit of cell membrane including leakage resistance R_L and series resistance R_s.

The parameter R is defined by

$$R = \frac{R_m R_L}{R_m + R_L}. \tag{7}$$

There are three cases to consider, i.e., $R_m \gg R_L$, $R_m \simeq R_L$, and $R_m \ll R_L$.

(*a*) $R_m \gg R_L$. In this case, R is virtually equal to R_L and Eq. 4 reduces to the following expression if we assume that $R_s < R_L$.

$$G_p = \frac{1/R_L + \omega C_m^2 R_s^2}{1 + (\omega\tau)^2}, \tag{8}$$

where time constant τ is given by $\tau = C_m R_s$. Therefore, G_p reduces to $1/R_L$ at low frequencies. This result indicates that we are unable to determine membrane conductance in this case. On the other hand, Eq. 3 reduces to

$$C_p = \frac{C_m [1 - (R_s/R_L)]}{1 + (\omega\tau)^2}. \tag{9}$$

At low frequencies, this equation simplifies to

$$C_p = C_m (1 - R_s/R_L). \tag{10}$$

Since R_s is of the order of 20–30 MΩ while R_L is more than 10 GΩ, the ratio R_s/R_L is negligibly small. Therefore, measured capacitance C_p correctly represents membrane capacitance even if leakage conductance is larger than membrane conductance as long as R_s/R_L is very small.

(*b*) $R_m \simeq R_L$. For this case, G_p and C_p at low frequencies are given by the following equations.

$$G_p = 1/(R_s + R) = 1/R \tag{11}$$

Because $R \gg R_s$ and

$$C_p = C_m R/(R_s + R) = C_m. \tag{12}$$

Therefore, in this case, membrane and leakage conductances are inseparable whereas measured capacitance is virtually equal to C_m.

(*c*) $R_m \gg R_L$. For this case, G_p and C_p at low frequencies are given by the following equations:

$$G_p = 1/R_m \tag{13}$$

$$C_p = C_m(1 - R_s/R_m). \tag{14}$$

The ratio R_s/R_m is a very small number and under these conditions, both G_p and C_p are very close to true membrane capacitance C_m and conductance G_m. It should be noted from these analyses that the presence of the leakage resistance R_L does not affect the measurement of membrane capacitance, whereas Eqs. 8 and 11 indicate that it is virtually impossible to measure membrane conductance if leakage conductance is larger than or comparable to membrane conductance. Only if leakage conductance is much smaller than membrane conductance can the latter be determined accurately. Despite this difficulty, we found, consistently, the membrane conductance of erythrocyte of the order of 6–7 $\mu S/cm^2$ at low frequencies. This value is similar to the one reported by Hunter (1977) and by Lassen et al. (1978) using different techniques. Therefore, we conclude that the magnitude of R_L is much larger than R_m and the error in measured membrane conductance due to leakage may not be as serious as we had expected.

For the conversion of measured capacitance and conductance to values per unit area, an accurate value of membrane area of erythrocyte is needed. The area of erythrocyte surface was estimated by Evans and Fung (1972) and Fung (1981) at various osmolarities. At the normal osmolarity an area of 135 μm^2 was found. Although Fung cites an even smaller value reported by Tsang (1975), we used an area of 135 μm^2.

Suspension Technique. Although the dielectric properties of erythrocyte suspension were studied by other investigators previously (Schwan and Carstensen, 1957), we needed more detailed data for the calculation of membrane capacitance. For these measurements, erythrocytes were suspended in a hypoosmotic phosphate buffer solution (½ of normal concentration) and measurements were carried out with preswollen cells. The effect of hypoosmotic condition on membrane permeability was studied using patch clamp technique. We were, however, unable to detect massive ion transports even under this condition. With this observation, we concluded that the mild hypoosmotic condition we used and subsequent swelling did not have noticeable effects on membrane conductance, particulary, on capacitance. The volume fraction was 43.8%. The dielectric constant and conductance of the suspension were measured between 50 KHz and 250 MHz using automated impedance analyzers (models 4191A and 4192A; Hewlett-Packard Co., Palo Alto, CA) with an on-line computer HP 9816. The conversion of dielectric constant and conductance of the suspension to membrane capacitance was performed using (*a*) Hanai–Asami–Koizumi's mixture theory (1969) and (*b*) the Maxwell Wagner equation (1892, 1914) for a sphere with a thin shell. Maxwell–Wagner mixture equation is given by Eq. 15.

$$\frac{\epsilon^* - \epsilon_a^*}{\epsilon^* + 2\epsilon_a^*} = \frac{\epsilon_c^* - \epsilon_a^*}{\epsilon_c^* + 2\epsilon_a^*} p, \tag{15}$$

where ϵ^* and ϵ_a^* are the complex dielectric constants of suspension and suspending medium. Volume fraction p is determined using the following equation:

$$p = \frac{2(1 - k_o/k_a)}{(2 + k_o/k_a)}, \tag{16}$$

where k_o is low frequency limiting conductivity and K_a is the conductivity of suspending medium. ϵ_c^* is the homogeneous dielectric constant of the particle averaged out for membrane and cell interior, ϵ_c^* is related to the dielectric

constants of membrane ϵ_m^* and cell interior ϵ_i^* by the following equation.

$$\frac{\epsilon_c^* - \epsilon_m^*}{\epsilon_c^* + 2\epsilon_m^*} = \frac{\epsilon_i^* - \epsilon_m^*}{\epsilon_i^* + 2\epsilon_m^*} V, \tag{17}$$

where

$$V = \left(\frac{R - d}{R}\right)^3 = \left(1 - \frac{d}{R}\right)^3, \tag{18}$$

where R is outer radius and d is membrane thickness. The dielectric constant of membrane can be calculated solving Eq. 15 for ϵ_m if the value of $\epsilon_i^*$is known. ϵ_i and k_i were determined from the high frequency limiting dielectric constant and conductivity. A value of 58 for ϵ_i and 5.2 mS/cm for k_i were found. These are very close to the estimate by Pauly and Schwan (1966). Once the value of ϵ_m is determined, membrane capacity C_m can be calculated by $C_m = \epsilon_m \epsilon_r / d$. The dielectric constant of membrane can also be calculated using Hanai–Asami–Koizumi (HAK) mixture equation instead of Eq. 15.

$$\frac{\epsilon^* - \epsilon_c^*}{\epsilon_a^* - \epsilon_c^*} \left(\frac{\epsilon_a^*}{\epsilon^*}\right)^{1/3} = 1 - p, \tag{19}$$

where volume fraction p is calculated using the following equation with the assumption that $k_m/k_a \ll 1$:

$$p = 1 - (k_o/k_a)^{2/3}. \tag{20}$$

The values of ϵ_c^* and ϵ_m^* are calculated, as for Maxwell–Wagner equation, using Eqs. 16 and 17. Computer programs used in these calculations handle complex quantities and compute the dielectric constant of membrane without analytically separating real and imaginary parts of complex dielectric constants.

RESULTS

Electrical properties, in general, can be displayed as resistance and reactance in the impedance presentation or capacitance and conductance in admittance presentation. Fig. 3 *A* illustrates the resistance and reactance of erythrocyte. This figure shows a very large reactance at low frequencies, hence a nearly 90° phase angle. This impedance diagram does not resemble those of nerve or muscle membranes which have a less than 90° phase angle. (Cole, 1986; Falk et al., 1964; Takashima and Schwan, 1974). *B* shows the impedance plot of a lipid bilayer lecithin membrane. The resemblance between these diagrams is striking. This indicates that erythrocyte membrane behaves nearly as a perfect dielectric material.

The capacitance of human erythrocyte is illustrated in Fig. 4 between 4 Hz and 10 KHz. These curves are the average of several measurements. Membrane capacitance shows a gradual decrease over a wide frequency range. At low frequencies, erythrocyte membrane has a capacity of 1.05 μF/cm^2. This value, however, decreases to 0.70

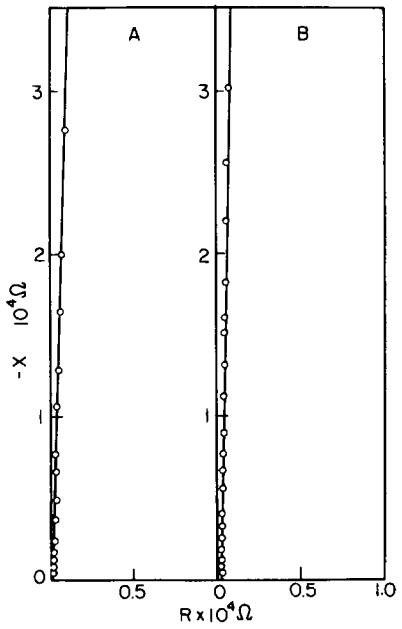

FIGURE 3 (*A*) Resistance and reactance of the erythrocyte membrane measured by micropipet method. (*B*) Resistance and reactance of a planar lecithin bilayer film. Note near 90° phase angle for both erythrocyte and lipid bilayer film.

μF/cm^2 at 10 KHz. The decrease of membrane capacitance may perhaps be partially due to the frequency dependence of electrode capacitance and may not reflect the properties of the erythrocyte membrane. Thus, we conclude that the capacity of the erythrocyte membrane is essentially independent of frequency. Fig. 5 shows membrane conductance between 4 and 300 Hz. The scale of the ordinate was greatly expanded in an attempt to determine the limiting value of membrane conductance at low frequencies. The curve, as shown, extrapolates to a value of <10 μS/cm^2 at low frequencies.

The high frequency limiting value of membrane capaci-

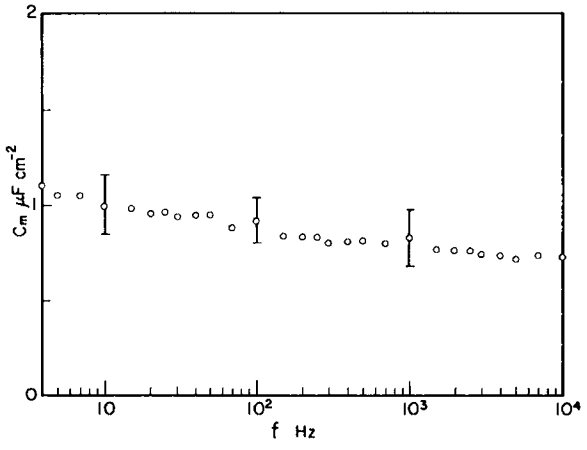

FIGURE 4 Frequency profile of the capacitance of erythrocyte. Capacitance ranges from 1.0 μF/cm^2 to 0.70 μF/cm^2 between 4 Hz and 10 KHz.

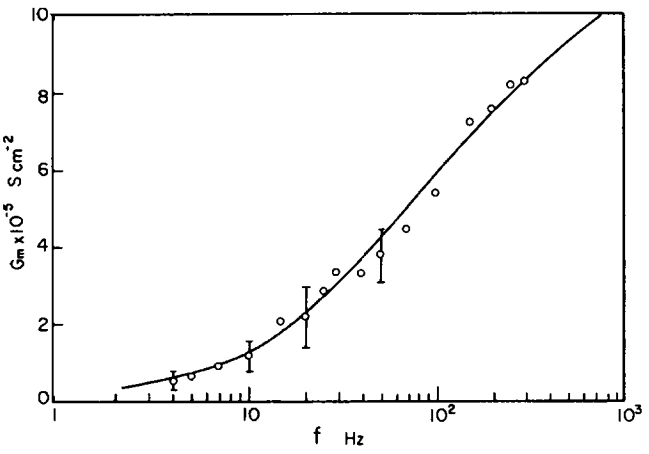

FIGURE 5 Low frequency limiting membrane conductivity with an expanded ordinate scale. Note that conductance is still decreasing at 4–5 Hz.

tance, as shown in Fig. 4, is 0.7–0.75 μF/cm^2. This value is comparable to the membrane capacitance determined by suspension techniques as discussed below. Fig. 6 shows the dielectric constant and conductivity of erythrocyte suspension. Membrane capacitance can be calculated using the Maxwell–Wagner equation or Hanai et al.'s equation as discussed earlier. For this calculation, only the low frequency dielectric constants and conductivities are used. The values of membrane capacitance calculated by Hanai et al.'s equation and those obtained by the Maxwell–Wagner theory are shown in Tables I and II along with the values obtained by micropipet technique. As shown, the membrane capacitance obtained by the Maxwell–Wagner theory are consistently higher than those obtained by the HAK equation. The latter gives the values of 0.65–0.7 μF/cm^2. The membrane capacitance obtained by the micropipet technique is of the order of 0.7–0.75 μF/cm^2.

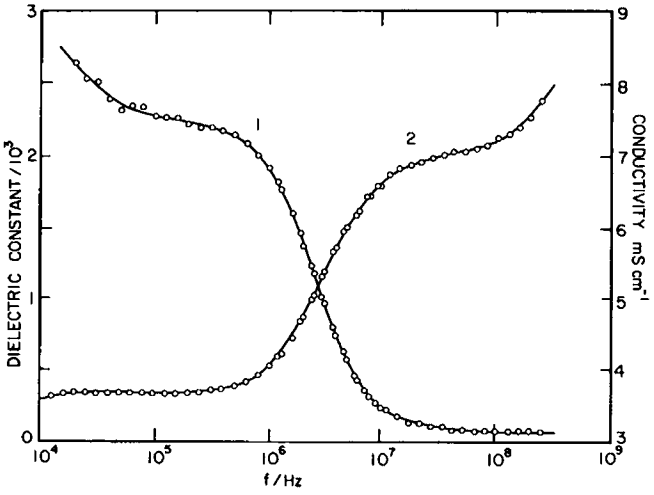

FIGURE 6 Dielectric constant (curve *1*) and conductance (curve *2*) of the suspension of erythrocytes. Volume fraction *P* is 43.8%. Osmolarity is ~150–200 mosmol.

TABLE I
MEMBRANE CAPACITANCE MEASURED BY MICROPIPET METHOD

Frequency	C_m
KHz	$\mu F/cm^2$
0.1	0.92
0.2	0.84
0.5	0.80
1.0	0.81
2.0	0.79
5.0	0.72
10.0	0.73

Although these values are subject to some uncertainty owing to the difficulty of accurately measuring electrode capacitance over the entire frequency range, the capacitances determined by the micropipet technique are similar to those obtained by HAK equations.

Another point of interest is the membrane conductance determined by micropipet technique. Previous research by Tosteson et al. (1973), Hunter (1977), and Lassen et al. (1978) indicate that the conductance of erythrocyte membrane is extremely small. Also recent time domain patch clamp measurements indicate an unusually small conductance of the erythrocyte unless the membrane is treated with Gardos effect inducing agents (Gardos, 1958; Hamill, 1981; Grygorczyk et al., 1984). Fig. 5, which shows the conductances of the erythrocyte membrane with an expanded scale, shows the low frequency conductance at 4 Hz to be ~10 μS/cm^2. The conductance will further decrease as the frequency decreases below 4 Hz and the curve seems to converge to a very low value of 5–6 μS/cm^2 asymptotically.

The voltage dependence of membrane capacitance is negligible unless a very large input potential of more than 200–300 mV is used. The membrane of the erythrocytes, therefore, behaves as a linear system.

DISCUSSION

Membrane Capacitance

The capacitance of the erythrocyte membrane was determined using (*a*) micropipet AC admittance method and

TABLE II
MEMBRANE CAPACITIES DETERMINED BY SUSPENSION METHOD

Frequency	HAK theory	Maxwell-Wagner Eq.
KHz	$\mu F/cm^2$	$\mu F/cm^2$
39.8	0.713	0.882
50.1	0.691	0.855
63.1	0.679	0.867
79.4	0.695	0.859
100	0.679	0.833
125	0.673	0.837
158	0.679	0.839
199	0.677	0.823

(*b*) conventional suspension technique. Although these techniques are entirely different in principle, the capacitances determined by these methods are, almost quantitatively, in agreement. The value obtained by suspension technique is 0.8 $\mu F/cm^2$ by the Maxwell–Wagner theory and 0.65–0.7 $\mu F/cm^2$ by Hanai et al.'s equation, whereas micropipet technique gives a value of 0.7–0.75 $\mu F/cm^2$. The capacitances measured by suspension technique were determined above 50 KHz. Owing to various difficulties, particularly electrode polarization and the dominance of interfacial polarization at low frequencies, the measurement with cell suspensions cannot be extended to the range below 50 KHz. These limitations, however, do not exist for micropipet technique and measurement can be extended to much lower frequency regions. As illustrated in Fig. 4, membrane capacitance increases gradually as frequencies decrease and reaches a value of ~ 1.05 $\mu F/cm^2$ at 4–5 Hz. The frequency dependence of membrane capacitance of passive biological cells has never been studied before. As clearly seen in this diagram, the capacitance of erythrocyte membrane does not exhibit a well-defined frequency dispersion. This is in contrast to the frequency-dependent membrane capacitance of nerve membranes (Takashima and Schwan, 1974).

Membrane Conductance

Another limitation of the suspension technique is its inability to measure the membrane conductance. In particular, the conductance of erythrocyte membrane is extremely small and, under these circumstances, suspension technique is simply incapable of detecting those near zero conductances. Even recent patch clamp measurements by Hamill (1981) and Grygorczyk et al. (1984) failed to detect gross current or single channel current with intact erythrocytes. Only when red cells are treated with Gardos effect inducing agents did these investigators observe single channel currents of the order of 2–3 pA. These results clearly indicate that erythrocyte membrane behaves almost like an insulator. The conductance observed by the present experiment is of the order of 10 $\mu s/cm^2$ at 4–5 Hz. By extrapolating the conductance curve shown in Fig. 5, we seem to obtain a limiting value of 5–6 $\mu S/cm^2$, including, perhaps, a small leakage conductance.

The subsequent paper will discuss the capacity and conductivity of the membranes of mouse lymphocytes.

Received for publication 27 April 1988 and in final form 1 July 1988.

REFERENCES

Asami, K., T. Hanai, and N. Koisumi. 1976. Dielectric properties of yeast cells. *J. Membr. Biol.* 28:169–180.

Cole, K. S. 1968. Membranes, Ions and Impulses. University of California Press, Berkeley, CA.

Evans, E., and Y. C. Fung. 1972. Improved measurements of the erythrocyte geometry. *Microvasc. Res.* 4:335–347.

Falk, G., and P. Fatt. 1964. Linear electrical properties of striated muscle fibres observed with intracellular electrodes. *Proc. R. Soc. Lond. B. Biol.* 160B:69–123.

Fung, Y. C. 1981. Red blood cells and their deformability. *Biomechanics.* Springer-Verlag, New York.

Gardos, G. 1958. The function of calcium in the potassium permeability of human erythrocytes. *Biochim. Biophys. Acta.* 30:653–654.

Grygorczyk, R., W. Schwarz, and H. Passow. 1984. Ca^{++}-activated K^+ channels in human red cells. Comparison of single-channel currents with ion fluxes. *Biophys. J.* 45:693–698.

Hamill, O. P. 1981. Potassium channel currents in human red blood cells. *J. Physiol. (Lond.).* 319:97–98.

Hanai, T., K. Asami, and N. Koizumi. 1979. Dielectric theory of concentrated suspensions of shell-spheres in particular reference to the analysis of biological cell suspensions. *Bull. Inst. Chem. Res.* 57:297–305.

Hille, B., and D. T. Campbell. 1976. An improved vaseline gap voltage clamp for skeletal muscle fibers. *J. Gen. Physiol.* 67:265–293.

Hunter, J. J. 1977. Human erythrocyte anion permeabilities measured under conditions of net charge transfer. *J. Physiol. (Lond.).* 268:35–49.

Julian, F. J., J. W. Moore, and D. E. Goldman. 1962. Current-voltage relations in the lobster giant axon membrane under voltage clamp conditions. *J. Gen. Physiol.* 45:1217.

Lassen, U. V., L. Pape, and B. Vestergaard-Bogind. 1978. Chloride conductance of the *Amphiuma* red cell membrane. *J. Membr. Biol.* 39:27–38.

Maxwell, J. C. 1892. Treatise on Electricity and Magnetism. Clarendon Press, Oxford.

Pauly, H., and H. P. Schwan. 1966. Dielectric properties and ion mobility in erythrocytes. *Biophys. J.* 6:621–639.

Sakmann, B., and E. Neher. 1983. Single Channel Recording. Plenum Publishing Corp., New York.

Schwan, H. P. 1957. Electrical properties of tissue and cell suspensions. *Adv. Med. Biol. Phys.* 5.

Schwan, H. P. 1963. Determination of biological impedance. *In* Physical Techniques in Biological Research. W. L. Nastuk, ed. Vol. 6. Academic Press, Inc., New York. 323–407.

Schwan, H. P., and E. Carstensen. 1957. Dielectric properties of the membrane of lysed erythrocytes. *Science (Wash. DC).* 125:985–986.

Takashima, S., and H. P. Schwan. 1974. Passive electrical properties of squid axon membrane. *J. Membr. Biol.* 17:51–68.

Tasaki, I. 1982. Physiology and Electrochemistry of Nerve Fibers. Academic Press, Inc., New York.

Tosteson, D. C., R. B. Gunn, and J. O. Wieth. 1973. Erythrocytes, Thromobocytes, Leukocytes. E. Gerlach, E. Moser, E. Deutsch, and W. Wilmanns, eds. Thieme, Stuttgart.

Tsang, W. C. O. 1975. The Size and Shape of Human Red Blood Cells. M.S. Thesis, University of California, San Diego.

Wagner, K. W. 1914. Erklarung der Dielektrischen Nachwirkungs Vorgange auf grund Maxwellscher Forstellungen. *Arch. Elek. Tech. (Berl.).* 2:371.